韓國海洋工學會誌 第11卷 第3號, pp.153~162, 1997. 8

◉ 論 文

Tide, Swash Infiltration and Groundwater Behavior

Hong-Yoon Kang* · Nobuhisa Kobayashi** · Cheong-Ro Ryu***

(97년 5월 30일 접수)

조석, 파랑의 침투와 지하수 거동

강 홍 윤* · 고바야시 노부히사** · 류 청 로***

Key Words : Infiltration (침투), Wave Runup (파랑의 쳐올림), Tide (조석), Groundwater(지하수), Beach (해안)

초 록

시간평균된 해안의 지하수위는 내륙쪽에 강우가 없는 경우에도 평균해수면 (Mean Sea Level)보다 1 내지 2미터 정도 높은 것으로 관측되었다. 이러한 해안의 지하수위상승현상은 주로 파랑과 조석의 작용에 의해 나타난다. 본 연구에서는 지하수위상승에 미치는 조석 및 파랑의 효과를 현장관측결과를 통해 정량적으로 보여주었으며, 또한 이들 각각의 작용에 기인한 지하수위상승에 대한 해석해 및 최근 이론들을 제시하였다. 특히, 최근 지하수의 수리학적 모델링에 관한 연구에서 파랑의 침투 (wave runup infiltration) 효과의 중요성이 강조되었는 바, 본 연구를 통해 종래에 보고된 바 없는 swash zone (shoreline 과 runup limit 사이) 에서의 파랑의 침투속도(분포)를 지하수위관측자료를 이용해 간접적으로 산정함으로써 해안의 지하수위예측모델링을 보다 정확히 수행할 수 있으리라 사료된다.

1. INTRODUCTION

Water infiltration from wave runup on a dry beach face during rising tides raises coastal watertable[1) 4)]. The interrelated phenomena of wave runup distributions, water infiltration/exfiltration and groundwater response have received relatively little attention although these interactions are important for hydrodynamics and sediment transport in the swash zone. Packwood[5)] analyzed the percolation of wave runup due to a single bore incident on an initially dry

* 정회원, Research Scholar, Center for Applied Coastal Research, University of Delaware, Newark, Delaware 19716, U.S.A.

** Professor and A. ociate Director, Center for Applied Coastal Research, University of Delaware, Newark, Delaware 19716, U.S.A.

*** 정회원, 부경대학교 해양공학부 교수

sandy beach numerically where he neglected partially-saturated sand. Nielsen et al.[2] appear to have been the first researchers that examined the distribution of wave runup and the velocity and nature of runup infiltration in the swash zone, and attempted to model watertable responses to waves and tides. Recently, Nielsen and Hanslow[6] analyzed wave runup distributions on natural beaches in relation to the infiltration velocity distribution, speculating that it would be proportional to the fraction of time during which the sand surface is under water. This speculation neglects the effect of the degree of beach saturation on the infiltration as will be shown in this paper. More recently, Turner[7,8] demonstrated the significance of tides and wave runup infiltration to grounwater superelevation.

Accurate modelling of the mean water surface and watertable near the shoreline will need to include wave runup infiltration/exfiltration processes on the time scale of individual waves[8,10] although no model apart from the highly idealizd simulation by Packwood[9] is available at present. Flow resistance and sediment transport on the beach face are also closely related to the beach permeability.

This paper presents a brief review of recent work on the coastal groundwater behavior driven by waves and tides, and the infiltration process linking wave runup to watertable overheight which may eventually be incorporated in a comprehensive watertable model.

2. COASTAL WATERTABLE BEHAVIOR

The watertable a few tens of meters landward of the high water mark on a beach can be considerably higher than the mean sea level (MSL) even if there is no outflow due to rainfall on the land[4,10]. This watertable overheight is partly due to waves and partly due to tides[7,8,10].

Fig. 1 illustrates coastal watertable processes associated with waves and tides. Several useful definitions are given below.

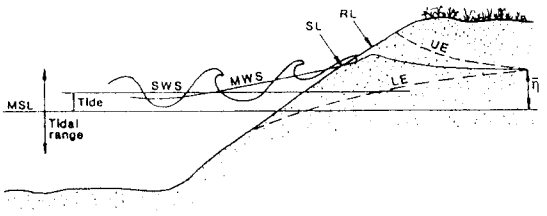

Fig. 1 Conceptual Sketch at Coastal Boundary

The long-term average level of the ocean surface outside the surf zone is the mean sea level (MSL). The still water surface (SWS) is the sea surface in the absence of waves. It varies vertically due to astronomical tides and changes in barometric pressure and winds. Local short-time (15 to 30 minutes) averaging of the water level defines the mean water surface (MWS) which intersects the beach at the shoreline (SL) and is connected to the watertable (WT). The mean water surface and watertable is not horizontal. Offshore of the breaking point it may be slightly below the still water surface due to wave set-down and inside the surf zone it rises towards the beach due to wave set-up. The watertable rises further landward of the shoreline. On a low tide, this rise may be caused partly by stored water from the previous high tide. On a rising tide, however, it is entirely due to the infiltration from wave runup, resulting in the humped shape of the watertable near the runup limit (RL). Landward of the high water mark (the runup limit at a high tide) the watertable oscillates within the upper and lower envelopes denoted by UE and LE in Fig. 1 which approaches an average superelevation $\overline{\eta}$ above the mean sea level. The ranges of different oscillations depend on their periods.

Wind waves, surf beats and even tides may not be felt more than a few tens of meters landward of the high water mark (HWM) but oscillations due to wave height changes over several days can reach further landward [2),4),11)].

Fig. 2 shows typical watertable profiles on high and low tides measured at the Kings Beach, Australia[12)]. The watertable profile at the low tide does not exhibit a hump, as opposed to the hump at the high tide. In other words, infiltration during the falling/low tides is normally negative and corresponds to outflow from the beach, in contrast to the positive infiltration into the beach during the rising/high tides.

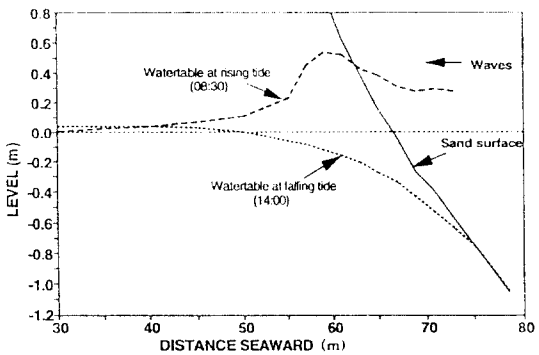

Fig. 2 Comparison of Watertables Measured on High and Low Tides (Kings Beach, Sept. 25, 1991)

3. TIDAL FORCING ON COASTAL GROUNDWATER

Tidal effects on the coastal watertable have been measured directly as indicated by "Pittwater Beach" data in Fig. 3. The simplest model for the watertable is based on the Dupuit-Forchheimer assumptions which neglect the capillary fringe. The resulting continuity equation coupled with the Darcy's law is called the Boussinesq equation

$$S_y \frac{\partial h}{\partial t} = K \frac{\partial}{\partial x}\left(h \frac{\partial h}{\partial x}\right) \qquad (1)$$

where h = local height of the watertable above a horizontal, impermeable base, K = constant hydraulic conductivity, S_y = specific yield, x = cross-shore horizontal coordinate taken to be positive landward, and t = time.

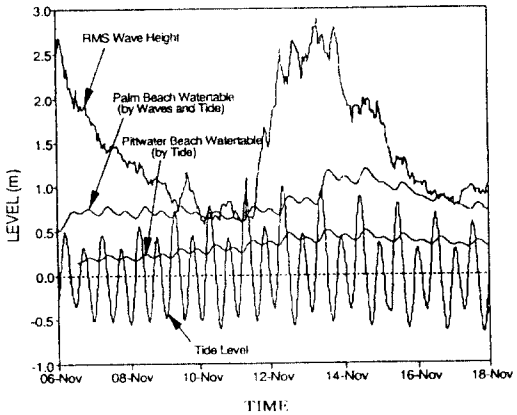

Fig. 3 Watertable Time Series from Exposed and Protected Sides of the Palm/Pittwater Beach Isthmus, Sydney, Australia. The watertable gauges at Palm Beach (exposed) and Pittwater Beach (protected) were of the order 10m landward of the respective high water marks. The watertable variation on the ocean side is larger when the root mean square (RMS) wave height is large because the wave setup brings "the action" closer to the well. The shape of the tidal signal transmitted to the watertable is skewed towards a sawtooth shape, and the watertable difference between the wells at the exposed and protected sides is seen to correlate with the RMS wave height

The oscillatory tidal motion can normally be explained on the basis of the following linearized form of the nonlinear equation (1)

$$S_y \frac{\partial h}{\partial t} = KD \frac{\partial^2 h}{\partial x^2} \qquad (2)$$

which assumes that the tidal amplitude A is much smaller than the constant aquifer depth D below MSL.

3.1 Oscillatory Solution

For the watertable motion corresponding to the tidal elevation η_{tide} above MSL with the amplitude A and the angular frequency ω given by

$$\eta_{tide} = A\cos\omega t \tag{3}$$

on a vertical beach at $x = 0$, the linearized equation (2) yields the following well-known analytical solution for the watertable elevation η above MSL[11]:

$$\eta(x, t) = A\, e^{-k_B x}\cos(\omega t - k_B x) \tag{4}$$

where k_B is the Boussinesq wave number given by

$$k_B = \sqrt{\frac{S_y\omega}{2KD}} \tag{5}$$

3.2 Overheight for Vertical Beach

The solution (4) yields zero mean $\overline{\eta}(x)=0$ everywhere and hence $\overline{h}(x)=D$ where the overbar denotes time-averaging. Philip[13] showed that the nonlinear nature of equation (1) leads to an overheight of the watertable which builds up asymptotically with increasing distance from the beach. This asymptotic overheight $\overline{\eta}_{nl}$ for the case of $A \ll D$ is given by

$$\overline{\eta}_{nl} = \frac{A^2}{4D} \tag{6}$$

for the vertical beach at $x=0$.

3.3 Overheight due to Sloping Boundary

Generally, the greatest tidal contribution to the watertable overheight inside the beach is due to the fact that the seaward boundary of the watertable is a sloping beach instead of a vertical wall.

Nielsen[11] has showed that if no seepage face is formed on the sloping beach, i.e., if the watertable is always able to keep up with the falling tide, the overheight due to the uniform slope with the angle β from the horizontal is given by

$$\overline{\eta}_{\beta} = 0.5\varepsilon A \tag{7}$$

which is based on a perturbation solution of the linearized equation (2) with a nonlinear seaward boundary condition and the small parameter ε defined as

$$\varepsilon = k_B A\cot\beta \tag{8}$$

3.4 Combined Overheight and Seepage Face Formation

Aseervatham et al.[10] and Aseervatham[14] extended the analytical work of Nielsen[11] by considering the combined effects of the sloping beach and the nonlinearity of equation (1) but found no terms proportional to $\varepsilon A(A/D)$. Consequently, the combined overheight is given by

$$\overline{\eta}_{\infty} = 0.5\varepsilon A + \frac{A^2}{4D} \tag{9}$$

which is the sum of the results of Philip[13] and of Nielsen[11]. Furthermore, Aseervatham et al.[10] obtained good agreement between equation (9) and Hele-Shaw cell experiments on relatively steep beaches.

The field data of Nielsen[11] has indicated that the watertable landward of the high water mark is higher than that predicted by equation (9) if the watertable can not keep up with the falling tide and a seepage face is formed above the low tide. The seepage face formation causes a difficulty in modeling the watertable. Turner[15] obtained reasonable agreements with his field

data using a simple model of Dracos[16] for the movement of the seepage exit point. However, Dracos's model is physically unsatisfactory because the maximum velocity for the exit point is assumed to be the same as a water particle seeping downwards along the slope without regard to the watertable dynamics landward of the exit point.

4. WAVE FORCING ON COASTAL GROUNDWATER

The groundwater flow pattern driven by the wave setup on the scale of the surf zone was illustrated and modelled by Longuet-Higgins[17] who neglected wave runup infiltration.

As indicated in Fig. 3, the watertable elevation varies on the time scale of hours corresponding to the changes of the height H, period T and direction of offshore wind waves[4]. The hydraulic conductivity K of the beach sand and the changing beach topography also affect the watertable fluctuations shown in Fig. 3 for the ocean side and protected side of a coastal barrier.

4.1 Regular Waves on Laboratory Beaches

Tidal effects and uncertainties associated with the sand characteristics and beach morphology can be eliminated by conducting laboratory experiments with regular waves as reported in some detail by Kang et al.[4].

The flume experiments using two sand sizes of the median diameter d_{50} = 0.18 mm and 0.78 mm conducted by Kang et al.[4] indicated that the ratio between the wave-generated overheight $\overline{\eta}_w$ and the runup height R above SWS for both sands was approximately given by

$$\frac{\overline{\eta}_w}{R} \simeq 0.62 \tag{10}$$

Furthermore, the measured runup height R was in good agreement with the formula proposed by Hunt[18] for regular waves on uniform slopes

$$R \simeq \sqrt{HL_o}\tan\beta_F \tag{11}$$

where the foreshore slope, $\tan\beta_F$, was used for beaches of variable slopes, H is the wave height on the horizontal bottom of the flume and L_o is the deep-water linear wave length given by

$$L_o = \frac{gT^2}{2\pi} \tag{12}$$

Substitution of equation (11) into (10) yields

$$\overline{\eta}_w \simeq 0.62\sqrt{HL_o}\tan\beta_F \tag{13}$$

4.2 Irregular Waves on Natural Beaches

The situation on natural beaches is more complicated partly because wind waves are irregular with respect to both period and height, and surf beats, i.e., oscillations with periods of the order 100 seconds may be dominant near the shoreline on gently sloping beaches[19,20].

Extracting the wave-generated overheight $\overline{\eta}_w$ from the total overheight $\overline{\eta}$ in the field is difficult because of the presence of tides. However, the data shown in Fig. 3 which contains data from the exposed and protected beaches with practically identical tides may allow one to separate the wave effect. Kang et al.[4] suggested that the watertable difference between the ocean side (Palm Beach) and the protected side (Pittwater Beach) might be approximately the same as the wave-generated overheight estimated by

$$\eta_{Palm\ Beach} - \eta_{Pittwater} \simeq 0.55\sqrt{H'_{orms}L_o}\tan\beta_F \tag{14}$$

where H'_{orms} is the equivalent unrefracted

offshore root-mean-square wave height and estimated as $H'_{orms} = (\cos\alpha_o)^{0.5} H_{orms}$ from the measured offshore wave height H_{orms} with α_o being the wave angle between the offshore wave crest and the shoreline. The wave period for L_o given by equation (12) was taken as the peak period. However, a better fit to the data presented in Fig. 7 of Kang et al.[4] instead of equation (14) is expressed as

$$\eta_{PalmBeach} - \eta_{Pittwater} \simeq 0.1 + 0.44\sqrt{H'_{orms} L_o}\tan\beta_F \quad (15)$$

where the constant 0.1 m in this equation may be attributed to the difference in the tide-generated overheight on the two sides or to the residual overheight generated by large waves during the subsequent period of small waves. More data are required to estimate the wave-generated overheight of the watertable inside natural beaches. Tentatively, the order of magnitude of the wave-generated overheight may be estimated as

$$\bar{\eta}_w \simeq 0.44\sqrt{H'_{orms} L_o}\tan\beta_F \quad (16)$$

for steep beaches ($\tan\beta_F > 0.1$) like Palm Beach illustrated in Fig. 3. This result is similar to the regular wave result given by equation (13), where the constant 0.44 in equation (16) could be adjusted by the use of different representative wave heights and periods. However, this adjustment is not warranted without additional field data.

Equation (16) derived from a set of steep beach data may not be applicable to gently sloping beaches where swash oscillations on such dissipative beaches are generally dominated by low-frequency waves[19,21].

5. INFILTRATION VELOCITY DISTRIBUTIONS

As mentioned earlier in relation to Fig. 2, the watertable inside a beach during a rising tide shows a hump due to water infiltration between the shoreline x_s and the runup limit x_R. This is due to the infiltration in the swash zone. Linearized equation (2) may be modified to include this infiltration effect as follows :

$$S_y \frac{\partial h}{\partial t} = KD\frac{\partial^2 h}{\partial x^2} + U_I(x,t) \quad \text{for } x_s \le x \le x_R \quad (17)$$

where U_I is the infiltration flow rate per unit horizontal area.

For the laboratory experiment without tidal effects, a quasi-steady state is reached after beaches are exposed to wave action of a sufficient duration. For the steady state, U_I is defined as the average infiltration velocity over wave periods and the time-averaged equation obtained from equation (17) can be written as

$$\frac{d^2 h}{dx^2} = -\frac{U_I(x)}{KD} \quad (18)$$

5.1 Steady Laboratory Conditions

Fig. 4 shows the normalized infiltration velocity distribution in the swash zone from the steady state laboratory data[4] with a fitted curve showing the trend of scattered data points. The infiltration velocity U_I is estimated indirectly from the measured watertables between the shoreline and the runup limit using equation (18) which is approximated by the following finite difference form

$$U_I(x) = -KD\frac{h(x-\delta_x) - 2h(x) + h(x+\delta_x)}{\delta_x^2} \quad (19)$$

where δ_x is the grid spacing. The values of K and D are found directly from the laboratory experiment[10]. The aquifer depth D in the flume

experiment is the height from the horizontal bottom to the still water level. The nondimensional horizontal coordinate X_n in Fig. 4 is defined as

$$X_n = \frac{x - x_s}{x_R - x_s} \tag{20}$$

where $X_n = 0$ at the shoreline $x = x_s$ and $X_n = 1$ at the runup limit $x = x_R$. The infiltration velocity U_I is normalized by the hydraulic conductivity K because the infiltration velocity of standing water of very small depth is approximately given by $U_I \simeq K$ on the basis of the vertically one-dimensional analysis of Philip[22].

Fig. 4 shows that U_I/K in the steady state has a maximum approximately halfway between the shoreline and runup limit. The dashed and dotted lines represent the infiltration velocity distribution for coarse and fine sands, respectively. The data points are too scattered to pinpoint the sand size effects on U_I/K. Equation (18) implies that U_I is the maximum at the location where the convex curvature of the watertable profile is the maximum.

Fig. 4 shows that the values of U_I/K in the swash zone are on the order of 0.1 and much less than the value of 1.0 expected for standing water. This suggests that the fraction of time during which the sand surface is under water may be important as speculated by Nielsen and Hanslow[6]. However, this fraction of wet time alone can not explain the convex distribution of U_I/K shown in Fig. 4 because the fraction of wet time decreases monotonically from the shoreline at $X_n = 0$ to the runup limit at $X_n = 1$. The other important factor affecting the infiltration velocity appears to be the void volume of the unsaturated sand absorbing the infiltrated water per unit horizontal area which is expected to increase monotonically from the shoreline to the runup limit. The combined effects of these opposing trends may explain the convex distribution shown in Fig. 4.

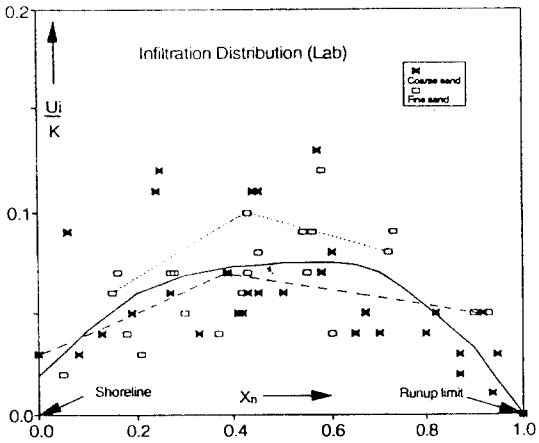

Fig. 4 Normalizd Infiltration Velocity Distribution as a Function of Normalized Cross-shore Distance in the Steady State. The solid line represents all data points, while the dotted and dashed lines represent the coarse and fine sands, respectively

5.2 Unsteady Field Conditions

Infiltration velocities for unsteady field conditions can be estimated by expressing the modified Boussinesq equation (17) in the following finite difference form

$$U_I(x,t) = S_y \frac{h(x,t+\delta_t) - h(x,t-\delta_t)}{2\delta_t} - KD \frac{h(x-\delta_x,t) - 2h(x,t) + h(x+\delta_x,t)}{\delta_x^2} \tag{21}$$

where δ_t is the time step size. Hence, the runup infiltration velocity $U_I(x,t)$ for unsteady conditions may also be estimated from the measured watertable heights and the parameters S_y, K and D of the porous medium. However, it is difficult to directly find the aquifer depth D for most field sites. The value of KD/S_y may be

estimated from the measured watertable heights $h(x,t)$ landward of the runup limit x_R where $U_I = 0$.

Substituting $U_I(x,t) = 0$ in equation (21) yields

$$\frac{KD}{S_y} = \frac{\delta_x^2}{2\delta_t} \frac{h(x,t+\delta_t) - h(x,t-\delta_t)}{h(x-\delta_x,t) - 2h(x,t) + h(x+\delta_x,t)} \quad (22)$$

The measured hydraulic conductivity K for beach sands is in the range of 10^{-5} - 10^{-3} m/s. The specific yield S_y for beach sands usually ranges between 0.23 and 0.28[23].

Table 1 KD/Sy Estimated for Five Field Sites

Field Sites	KD/S_y [m²/sec]
Kings Beach, Queensland	1.50 x 10^{-2}
Eagers Beach, Queensland	1.14 x 10^{-2}
Shelley Beach, Queensland	4.79 x 10^{-2}
Brunswick Beach, New South Wales	1.17 x 10^{-2}
Bribie Island North, Queensland	2.10 x 10^{-3}

Table 1 lists the values of KD/S_y estimated using equation (22) for five field sites along the east coast of Australia[12]. For the measured values of K and S_y at each site, the value of D at each site is thus estimated. The estimated values of D at these sites are about 15 m.

Fig. 5 shows the normalized infiltration velocity distribution U_I/K as a function of the relative cross-shore distance X_n for the unsteady field conditions. The data plotted in the figure represent typical infiltration velocities during the rising/high tides for the five beaches listed in Table 1. The solid curve shows a smoothed fitted line of the scattered data points. The normalized infiltration velocity for the natural beaches also has a maximum approximately halfway between the shoreline and the runup limit as in Fig. 4 for the steady state laboratory data. The dashed and dotted lines in Fig. 5 represent specific data sets from Kings Beach and North Bribie Island[12], respectively. Both the infiltration velocity distributions in the laboratory and the field show similar trends as shown in Figs. 4 and 5, but the magnitudes of U_I/K are different. This difference is perhaps due to the fact that the field data were taken during rising tides where the beach is less saturated than in the steady state of the laboratory experiments. Moreover, swash zones on natural beaches are generally wider for irregular wind waves and low-frequency waves in the field. The wider swash zone may increase the pore volume of the unsaturated beach sand above the saturated watertable.

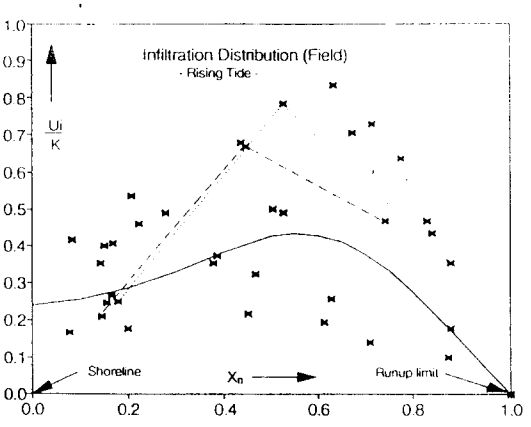

Fig. 5 Relative Infiltration Velocity Distribution as a Function of Normalized Cross-shore Distance for Unsteady Field Conditions

6. CONCLUSIONS

A concise review on tidal and wave effects on the coastal watertable has been presented to summarize the current understanding of physical

processes involved in coastal watertable-tide -wave interactions.

An emphasis has been placed on complex infiltration processes linking wave runup to watertable superelevation. Infiltration velocities between the shoreline and the runup limit are indirectly estimated from watertable data using the modified Boussinesq equation. The estimated infiltration velocities indicate that there is little difference in the magnitude and spatial distribution of the infiltration velocity between fine and coarse sand beaches in the laboratory experiments. The infiltration velocity U_I with its maximum value roughly midway between the shoreline and the runup limit for both the laboratory and field data has been estimated to be on the order of $0.1K$ for laboratory beaches and $0.5K$ for natural sand beaches. This difference may be related to the degree of saturation of beach sands as well as the degree of swash oscillations due to regular and irregular waves[21].

A numerical model including swash dynamics, infiltration into unsaturated sand, and watertable dynamics will be required to elucidate these complex interactions. Numerical models for very porous rubble structures with no unsaturated zone have already been developed[24].

ACKNOWLEDGEMENTS

This research has been supported by the Research Center for Ocean Industrial Development (RCOID), Korea while the first author is working at the Center for Applied Coastal Research, University of Delaware, USA.

REFERENCES

1) Wadell, E., "Swa[illegible] groundwater-beach profile interactions", *Soc. Econ. Paleontol. Mineral. Special Publication #24*, pp. 115-125, 1976

2) Nielsen, P., Davis, G.A., Winterbourne J. and Elias G., "Wave setup and the watertable in sandy beaches", *Tech. Rep.* 88/1, NSW Public Works, Aus., 132 pp., 1988

3) Hegge B.J. and Masselink G., "Groundwater-table responses to wave runup: an experimental study from Western Australia", *J. Coastal Res.*, Vol. 7, No. 3, pp. 623-634, 1991

4) Kang, H.Y., Nielsen, P. and Hanslow, D.J., "Watertable overheight due to wave runup on a sandy beach", *Proc. 24th Int. Conf. Coastal Eng.*, ASCE, Kobe, pp. 2115-2124, 1994

5) Packwood, A.R., "The influence of beach porosity on wave uprush and backwash", *Coastal Eng.*, Vol. 7, No. 1, pp. 29-40, 1983

6) Nielsen, P. and Hanslow, D.J., "Wave runup distributions on natural beaches", *J. Coastal Res.*, Vol. 7, No. 4, pp. 1139-1152, 1991

7) Turner, I.L., "A field study examining the practical significance of tides and waves to groundwater investigation in the coastal zone", *NSW Public Works, Technical Report* No. 95031, 125 pp., 1995

8) Turner, I.L., "Tides, waves and the super-elevation of groundwater at the coast", *J. Coastal Res.*, Vol. 13, No. 1, pp. 46-60, 1997

9) Li, L., Barry, D.A. and Pattiaratchi, C.B., "Modeling coastal ground-water response to beach dewatering", *J. Waterway, Port, Coastal and Ocean Eng.*, Vol. 122, No. 6, pp. 273-280, 1996

10) Aseervatham, A.M., Kang, H.Y. and Nielsen, P., "Groundwater movement in beach water-tables", *Proc. 11th Aust. Conf. Coast. Ocean Eng.*, IEAust, Townsville, pp. 589-594, 1993

11) Nielsen, P., "Tidal dynamics of the water-table in beaches", *Water Resources Res.*, Vol. 26, No. 9, pp. 2127-2134, 1990

12) Kang, H.Y., Aseervatham, A.M. and Nielsen, P., "Field measurements of wave runup and the beach watertable", *Res. Rep.* No. 148, Dept. Civil Eng., Univ. Queensland, Aus., 44 pp., 1994

13) Philip, J.R., "Periodic non-linear diffusion: an integral relation and its physical consequences", *Aust. J. Physics*, 26, pp. 513-519, 1973

14) Aseervatham, A.M., "Tidal dynamics of the coastal watertable", *Ph.D. Thesis*, Dept. Civil Eng., Univ. Queensland, Australia, 253 pp., 1994

15) Turner, I.L., "Watertable outcropping on macrotidal beaches: A simulation model", *Marine Geology*, Vol. 115, pp. 227-238, 1993

16) Dracos, T., "Ebene nichtstationare Grundwasserabflusse mit freier Oberflache", *Mitt. Versuchsanst. Wasserb Erdbau, Eidgenoss. Tech Hochsch*, Zurich, Rep., 57, 114 pp., 1962

17) Longuet-Higgins, M.S., "Wave setup, percolation and undertow in the surf zone", *Proc. Royal Society of London*, Vol. A390, pp. 283-291, 1983

18) Hunt, I.A., "Design of seawalls and breakwaters", *J. Waterway, Port, Coastal and Ocean Eng.*, Vol. 85, No. 3, pp. 123-152, 1959

19) Guza, R.T. and Thornton, E.B., "Swash oscillations on a natural beach", *J. Geophys. Res.*, Vol. 87, No. C1, pp. 483-491, 1982

20) Holman, R.A. and Sallenger, A.H., "Setup and swash on a natural beach", *J. Geophys. Res.*, Vol. 90, No. C1, pp. 945-953, 1985

21) Kobayashi, N. and Wurjanto, A., "Irregular wave setup and runup on beaches", *J. Waterway, Port, Coastal and Ocean Eng.*, Vol. 118, No. 4, pp. 368-386, 1992

22) Philip, J.R., "The theory of infiltration: 6. Effect of water depth over soil", *Soil Sci.*, 85, pp. 278-286, 1958

23) Johnson, A.I., "Specific yield-compilation of specific yields for various materials", *US Geology Survey Water Supply* Paper 1662-D, 74 pp., 1967

24) Wurjanto, A. and Kobayashi, N., "Irregular wave reflection and runup on permeable slopes", *J. Waterway, Port, Coastal and Ocean Eng.*, Vol. 119, No. 5, pp. 537-557, 1993